AD-A042 501 NAVAL RESEARCH LAB WASHINGTON D C F/G 4/1
OBSERVATIONS OF ELECTRON TEMPERATURE GRADIENTS IN MID-LATITUDE --ETC(U)
JUN 77 E P SZUSZCZEWICZ, J C HOLMES

UNCLASSIFIED NRL-MR-3345-REV NL

| OF |
AD A042501

END
DATE FILMED
8-77
DDC

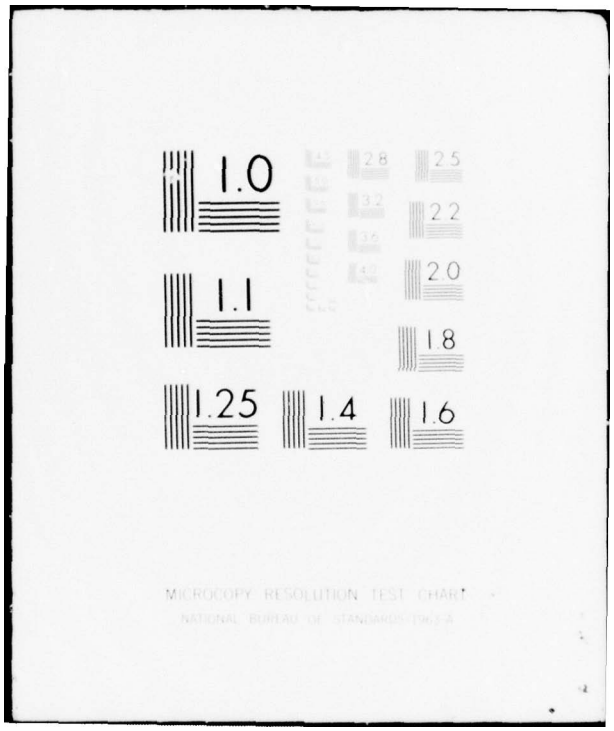
1.0
1.1
1.25
1.4
1.6
2.8
2.5
3.2
2.2
3.6
2.0
4.0
1.8
MICROCOPY RESOLUTION TEST CHART
NATIONAL BUREAU OF STANDARDS-1963-A

AD A042501

NRL Memorandum Report 3345
Revised

12
NW

Observations of Electron Temperature Gradients in Mid-Latitude E_s-Layers

EDWARD P. SZUSZCZEWICZ AND JULIAN C. HOLMES

Upper Air Physics Branch
Space Science Division

June 1977

DDC
RECEIVED
AUG 8 1977
C

NAVAL RESEARCH LABORATORY
Washington, D.C.

Approved for public release; distribution unlimited.

AD No.
DDC FILE COPY

SECURITY CLASSIFICATION OF THIS PAGE (When Data Entered)

REPORT DOCUMENTATION PAGE

READ INSTRUCTIONS BEFORE COMPLETING FORM

1. REPORT NUMBER
NRL Memorandum Report 3345 (Revised)

2. GOVT ACCESSION NO.

3. RECIPIENT'S CATALOG NUMBER

4. TITLE (and Subtitle)
OBSERVATIONS OF ELECTRON TEMPERATURE GRADIENTS IN MID-LATITUDE E_s-LAYERS

5. TYPE OF REPORT & PERIOD COVERED
Interim report on a continuing NRL problem

6. PERFORMING ORG. REPORT NUMBER

7. AUTHOR(s)
Edward P. Szuszczewicz and Julian C. Holmes

8. CONTRACT OR GRANT NUMBER(s)

9. PERFORMING ORGANIZATION NAME AND ADDRESS
Naval Research Laboratory
Washington, D.C. 20375

10. PROGRAM ELEMENT, PROJECT, TASK AREA & WORK UNIT NUMBERS
NRL Problem A02-11
Subtask RRD33-02-42

11. CONTROLLING OFFICE NAME AND ADDRESS

12. REPORT DATE
June 1977

13. NUMBER OF PAGES
41

14. MONITORING AGENCY NAME & ADDRESS(if different from Controlling Office)

15. SECURITY CLASS. (of this report)
UNCLASSIFIED

15a. DECLASSIFICATION/DOWNGRADING SCHEDULE

16. DISTRIBUTION STATEMENT (of this Report)
Approved for public release; distribution unlimited.

17. DISTRIBUTION STATEMENT (of the abstract entered in Block 20, if different from Report)

18. SUPPLEMENTARY NOTES

19. KEY WORDS (Continue on reverse side if necessary and identify by block number)
Ionosphere
Electron temperature
Plasma probe
Sporadic-E

20. ABSTRACT (Continue on reverse side if necessary and identify by block number)

Using a newly-developed pulsed plasma probe, direct measurements of electron temperature were performed within mid-latitude sporadic-E layers above White Sands, New Mexico. The probe's capability for unfolding density variations from its current-voltage characteristic made the temperature measurements possible within the steep density gradients characteristic of E_s layers. The major feature of the observations was the presence of an electron temperature gradient across the layers: the bottom-sides of the layers were isothermal at T_e = 340°K while the topside of each layer showed → next

(Continues)

DD FORM 1 JAN 73 1473 EDITION OF 1 NOV 65 IS OBSOLETE
S/N 0102-014-6601

SECURITY CLASSIFICATION OF THIS PAGE (When Data Entered)

251950

20. Abstract (Continued)

T_e increasing from 380° to more than 500°K over a vertical extent of 400 meters. The results are discussed in terms of reversible heating by gravity waves, as well as in terms of plasma density and ion composition effects within the ionospheric plasma itself.

CONTENTS

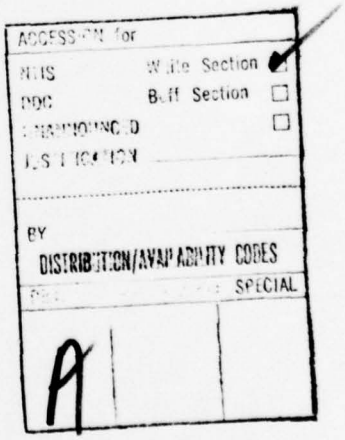

OBSERVATIONS OF ELECTRON TEMPERATURE GRADIENTS IN MID-LATITUDE E_s -LAYERS

I. INTRODUCTION

The underlying mechanism for the formation of mid-latitude sporadic-E layers by the convergence of metallic ions to wind shear nodes (Axford, 1967; Macleod, 1966; Whitehead, 1967) is found to account for much of the observed data (Matshushita and Smith, 1972 and 1975). However, the temperature predictions of individual particle populations in and near the layers (Hines, 1965; Gleeson and Axford, 1967; Hooke, 1969a,b) have not been fully tested, largely as a result of inadequacies in diagnostic devices or complementarity of payload instrumentation.

The work of Gleeson and Axford (1967), and Hooke (1969) describe the processes that determine charged-particle temperatures at E-region altitudes, and they employed their results to estimate the influences of electron density and ion composition on height variations of plasma temperatures in mid-latitude sporadic-E layers. They predict minima in both T_e and $(T_e - T_n)$ within the layer, with bottomside values substantially lower than the topside (Hooke, 1969a). The two cases described in detail

PRECEDING PAGE BLANK-NOT FILMED

by Hooke show that topside electron temperature can exceed that at the layer peak by at least 150°K whereas the electrons on the bottomside can be isothermal (within 10°K). In the work of Hooke, allowances were made for variations in the neutral gas temperature that can accompany tidal and gravity-wave motions. He clearly shows that variations in T_n can play a major role in the final height variation of electron and ion temperature through E_s layers.

In contrast to the works of Gleeson, Axford, and Hooke, which allow $T_e \neq T_n$, is the position that all particles below 130 km are in thermodynamic equilibrium, where variation in the temperature of the neutral species is accompanied by identical variations in the temperature of the charged particle population. To couple this concept with a proposed mechanism of reversible heating by gravity waves and tides (Hines, 1965; Hooke 1969 a,b) requires that changes in T_e cross an E_s layer be identified with the T_n variation produced by the gravity waves.

In this work we present pulsed-plasma-probe measurements of electron temperature which show that substantial temperature gradients do exist within an E_s -layer. This data was collected aboard an Aerobee 150 rocket launched from White Sands Missile Range on 29 June 1974 at 2031 MST. The payload reached an altitude of 229.5 km and up- and downleg portions of the flight passed through blanketing sporadic-E layers centered at 106.7 and 106.1 km,

respectively. The layers are shown in Figure 1 where the flight profiles of relative electron density are measured by peak electron currents collected by the probe. The up- and downleg E_s thicknesses at the 0.1 N_e^{max} point were 1.16 and .73 km with corresponding peak electron densities of $3(10^5)$ and $7(10^5)$ cm^{-3}, respectively.

Within the E_s layers, the probe simultaneously measured changes in ambient plasma density and electron temperature with a spatial resolution of 14 and 300 meters, respectively. This capability made temperature measurements possible within the steep density gradients characteristic of sporadic-E. This paper concentrates on these temperature results, showing that the E_s peak and bottomside values of T_e were approximately equal at 340^oK but with the topsides showing T_e enhancements with gradients as high as $340^oK/km$. Before discussing the details of these measurements and their implications with regard to theoretical concepts, we describe the experimental technique and analysis procedure.

II. EXPERIMENTAL TECHNIQUE

The instrument. A pulsed-plasma-probe (referred to as P^3) was utilized for the simultaneous measurements of electron density, temperature, and density variations. The P^3 is a Langmuir-type probe with a specialized electronic procedure for generating current-voltage characteristics

in a way which results in improved reliability and expanded versatility in laboratory, ionospheric and reentry plasma studies (Holmes and Szuszczewicz, 1975; Szuszczewicz and Holmes, 1975; 1976a,b). Compared with conventional Langmuir probe procedures, the P^3 technique reduces substantially the errors that can affect determinations of electron densities and energy distribution functions when probe surface conditions change within the measurement period (Hirao and Oyama, 1972; Sturges, 1973; Szuszczewicz and Holmes, 1975; Wehner and Medicus, 1952). P^3 diagnostic capabilities extend into the domain of temporal and spatial plasma variations where the technique additionally provides a simultaneous measurement of density fluctuation power spectrum and demonstrates itself as an important device for in situ investigations of irregular ionospheric structures.

The probe was a straight 16.4 cm length x 0.06 cm diameter tungsten wire extended from the payload tip on a 57 cm long boom electrically tied to the rocket potential. The probe was separated from the boom by a cylindrical guard electrode of 1.6 cm length, and both the probe and the guard electrode were swept with identical electric potentials of the form shown in Fig. 2 and specified by the parameters

$$\tau_s = 380 \text{ msec}$$

$$(\tau_{on}, \tau_B) = (100\mu s, 1900\ \mu s)$$

$$(V_-, V_+) = (-2.38v, +3.02v)$$

$$V_B = 0 \text{ v} \quad .$$

As shown in the figure, two alternating modes of probe operation were employed. Figure 2A depicts a linear sawtooth voltage which represents the conventional approach to Langmuir probe operation while Fig. 2B shows the pulse-modulated sweep utilized in the P^3 technique. The latter mode employs a sweep of pulses which follows a sawtooth envelope. Between pulses the sweep returns to a constant baseline voltage V_B. The sequence of four pulses generates four distinct I-V data points for the probe's current-voltage characteristic. The fifth pulse is blanked out so that the current I_B collected by the probe during the inter-pulse period can be monitored and used as a measure of variations in the probe-plasma system. These variations might include changes in the probe-s surface condition, plasma fluctuations, or rapid variations in plasma density as seen by a rocket or satellite passing through an in-homogenous ionospheric structure. The values for τ_{on} and τ_B (inset Fig. 2) were chosen to stabilize probe surface conditions (Holmes and Szuszczewicz, 1975; Szuszczewicz and Holmes, 1975) and establish I_B as a direct measure of plasma density variations. Additionally, the ratio of

reference electrode area (payload plus rocket body) to that of the sum of the probe and its guard was sufficiently large ($\sim 2(10^4)$) to guarantee that area effects (Szuszczewicz, 1972) would not perturb the measurement procedure. The arrangement of electrical parameters in the 5-pulse format allowed the sampling of baseline current I_B every 9.75 msec while a complete I-V characteristic was generated in 380 msec.

Analysis procedure. For a probe operating in the collisionless regime with applied electrical potentials less than that of the ambient plasma, the current-density response can be written as

$$j = N_e e \sqrt{\frac{kT_e}{2\pi m_e}} \left[\exp(\chi_p) - \sqrt{\frac{m_e}{M_i}} I_i(\beta, \tau, \chi, \alpha) \right] \quad (1a)$$

$$\equiv j_e + j_i \quad , \quad (1b)$$

where χ_p is the normalized difference between the probe and plasma potentials, V_p and V_o respectively; that is

$$\chi_p = e(V_p - V_o)/kT_e \quad . \quad (2)$$

β is the probe radius R_p divided by the electron Debye length λ_D, τ is the ratio of ion-to-electron temperature T_i/T_e, m_e is the mass of an electron, M_i is the charged-normalized ion mass $M_i = m_i/Z^2$, and I_i is the dimensionless ion current defined by

$$j_i = N_e e \sqrt{kT_e/2\pi m_i} \; I_i . \quad (3)$$

In Eqs. (1a) and (3) the quantities as yet undefined are the magnitude of charge of an electron e, the Boltzmann constant k, the experimentally observed ion-current density collected by the probe j_i, and the probe area α which collects "effective ion currents" as a result of bulk plasma flow or photoelectron emission. If plasma flow or photoemission effects are insignificant, I_i can be taken from the work of Laframboise (1966), otherwise a dimensionless form of the results of Wharton and Hoegy (1971) can be applied.

If plasma parameters are constant, standard analysis procedures (Chen, 1965; Boyd, 1968) can be applied to Eq. (1a) in order to determine the electron temperature and density. The procedure involves subtraction of the j_i component from j to empirically determine $j_e(V_p)$, the first term on the right in Eq. (1). Electron temperature is determined from the slope of the $\ln(j_e)$ vs V_p plot according to the relationship

$$T_e = \frac{e}{k}\left[\frac{d(\ln j_e)}{dV_p}\right]^{-1} . \qquad (4)$$

For probe potentials greater than that of the plasma ($\chi_p > 0$) electron current will dominate, and the current density to cylindrical electrodes can be represented by (Chen, 1965)

$$j_e(\chi_p>0) = N_e e \sqrt{\frac{kT_e}{2\pi m_e}}\left(\frac{2}{\sqrt{\pi}}\right)\left[\chi_p^{\frac{1}{2}} + g(\chi_p^{\frac{1}{2}})\right] \qquad (5)$$

where

$$g(\chi_p^{\frac{1}{2}}) = \sqrt{\frac{\pi}{2}} \exp(\chi_p) \left[1 - \mathrm{erf}(\chi_p^{\frac{1}{2}})\right] \tag{6}$$

and

$$\mathrm{erf}(\chi_p^{\frac{1}{2}}) = \sqrt{\frac{2}{\pi}} \int_o^{\chi_p^{\frac{1}{2}}} \exp(-t^2)\, dt \quad . \tag{7}$$

For $\chi_p \geq 4$ and $\chi_p \geq 10$, Eq. (5) may be written as

$$j_e \ (\chi_p \geq 4) = \left(\frac{2N_e e}{\sqrt{\pi}}\right) \sqrt{(kT_e/2\pi m_e)\ (1 + \chi_p)} \tag{8}$$

and

$$j_e(\chi_p \geq 10) = \sqrt{2/\pi^2 m_e}\ \ N_e e^{3/2} (V_p - V_o)^{1/2} \quad , \tag{9}$$

respectively. An identical procedure can be carried out for spherical probes with appropriate relationships substituted for Eqs. (5), (8) and (9). Experimentally, the electron density is determined by the slope of the appropriate portion of the I-V characteristic that applies to either Eq. (8) or (9). The latter has the advantage of T_e-independence.

If the electron density varies, T_e and N_e can be determined in the P^3 technique by unfolding the density fluctuations from Eqs. (1), (4), (8) and (9). This is done with interpulse measurements of I_B carried out at a fixed potential V_B while the net I-V characteristic is collected along the sawtooth envelope shown in Fig. 2B. Selecting

V_B so that I_B is insensitive to T_e (e.g. at $\chi_p \gg 1$), one can write

$$N_e = KI_B \quad . \tag{10}$$

Density-normalized probe characteristics can then be reconstructed from the raw data by substituting N_e^{ref} for N_e everywhere in Eqs. (1) through (9), with

$$N_e^{ref} = N_e(\bar{r},t)\left[\frac{I_B^{ref}}{I_B(\bar{r},\ t)}\right] \quad . \tag{11}$$

In practice, this procedure involves the multiplication of raw current values on the characteristic by the ratio $I_B^{ref}/I_B(\bar{r},t)$. The result is a current-voltage characteristic referenced to a constant plasma density N_e^{ref}. The selection of I_B^{ref} is arbitrary but generally takes on one of the I_B-values collected during the generation of the I-V characteristic being analyzed.

It should be pointed out that the plasma current collected by a probe has a number of subtle responses to density variations which were not discussed above. One of these subtleties is the effect of density on the value of β and its associated influence on I_i. This effect is noted here only for purposes of completeness because the probe's β-variations throughout the entire flight were in the orbital-motion-limited regime (Chen, 1965; Laframboise, 1966) and therefore did not alter the current response.

This was not necessarily the case for the reference electrode (the payload and rocket) which operated in the regime $10 \lesssim \beta \lesssim 100$. Reference electrode variations in β would change its collected ion current j_i and ultimately its floating potential. It has been shown (Szuszczewicz, 1972) that such a β-variation might result in a change in the vehicle's floating potential equivalent to $\sim 0.4kT_e/e$ volts. Variations of this nature were not present in the sporadic-E application reported here.

III. RESULTS

The payload was launched from White Sands Missile Range (32° 30'N, 106° 20'W), New Mexico, on 29 June 1974, at 2031 MST (0331 GMT, 30 June 1974) and reached an apogee of 229.5 km. The probe was deployed upleg at 102 km and last observed ionospheric plasma on reentry at 90 km. Figure 1 shows the up- and downleg profiles of relative electron density derived from the probe's saturation electron current collected at the maximum positive sweep voltage V^+. These profiles locate the up- and downleg E_s-layers at 106.7 and 106.1 km, respectively. Within the layers the probe operated in the pulse-modulated mode (Fig. 2B), providing each complete I-V characteristic with running measurements of relative plasma density every 14 meters.

Figure 3 is an expanded view of P^3 currents and voltages as the payload traversed the E_s-layer on the upleg portion of the flight. Plotted as a function of altitude are the net ion- I_p^i and electron I_p^e currents collected by the probe during voltage pulses which followed the sawtooth envelope (Fig. 2B). The baseline current values I_B are also shown and represent samples of relative plasma density. Since the probe's floating potential was approximately 1 volt positive with respect to that of the payload (the reference electrode) I_B samples at V_B=0 volts were collected in the ion-saturation portion of the I-V characteristic at a potential approximately equivalent to $-25kT_e/e$ volts relative to the ambient plasma potential.

Because plasma density is a rapidly changing function of altitude within the layers, the currents I_i^p and I_e^p were dependent upon the local density N_e as well as the voltage applied to the probe V_p. With I_B providing a measurement of variations in N_e, the $I_e(V)$ characteristic was unfolded from the $I_e(V,N_e)$ data by the method outlined in the previous section. Then the ambient electron temperature T_e was determined in the retarding-field region of the probe's characteristic (see Eq. (4)). For each I-V curve, I_B^{ref} was taken to be that value of I_B closest (in time) to the point where $I_i^p=I_e^p$. The value determined for T_e was ascribed to that referenced position, that is, the time and altitude of the floating potential (defined by $I_i^p=I_e^p$).

Results on the upleg trajectory yielded (T_e, Z) = (340° K, 106.4km), (345° K, 106.7km), 380° k, 107.5km) and (515° K, 107.9km) with the last measurement made outside the highest density region of the layer shown in Fig. 3.

Identical procedures were followed on the downleg passage through an E_s layer with the expanded-scale currents and voltages shown in Fig. 4. Only two downleg measurements were made, yielding (T_e, Z) = (345° K, 105.75km) and (500° K, 106.52km). The values of temperature and altitude shown within parentheses in Fig. 4 are those measured in the upleg E_s-layer and superimposed on the downleg profile by normalizing to identical ratios of $N_e(Z)/N_e(\text{peak})$. Because of limitations imposed by electrometer sensitivity, reliable measurements of electron temperature were not made in the trough region (109km $\leq Z \leq$ 200 km) above the E_s-layers. Above 200 km, values of electron temperature were between 850° and 1000° K.

Within the layers absolute values for $N_e(Z)$ were determinable from the slope of the density-normalized saturation portion of the I-V characteristics appropriate to Eq. (9). This analytical technique yielded electron densities of $3(10^5)$ and $7(10^5)$ cm^{-3} at the peaks of the up- and downleg layers, respectively. All other values of N_e within the layers can be scaled from the I_B-profiles in Figures 3 and 4.

The difference in layer thicknesses (1.16km upleg, 0.73km downleg) is in agreement with the generally systematic downward motion of E_s-layers accompanied by the profile growing thinner and more intense (Layzer, 1972). If in fact the up- and downleg observations were of the same layer (the horizontal separation between up- and downleg E_s-layer measurements was 60 km), the average downward drift velocity was equivalent to 1.8 m/sec.

The major feature of our E_s observations is the measurement of rather steep electron temperature gradients across the layers shown in Figures 3 and 4. The results show the bottom side of the layer as isothermal at $T_e \approx 345^\circ$K while the topside is accompanied by a positive gradient in T_e, resulting in an electron temperature of 515°K at the top edge of the layer. This is believed to be the very first detailed observation of electron temperature gradients within temperate latitude sporadic-E layers. Previous attempts at direct T_e determinations (Smith, 1966; Aubrey, et al, 1966) whithin E_s -layers were not as detailed as the results which we present here.

IV. DISCUSSION OF RESULTS

a. Coupling to Gravity Waves

In this section we consider the implications of our results from two points of view. The first assumes total thermodynamic equilibrium in the charged and neutral particle populations. There is support for this position ($T_e=T_i=T_n$) in incoherent radar scatter investigations of the daytime ionosphere in the undisturbed region (no E_s) below 130 km (Carru et al, 1967a,b· Evans, 1967· Wand and Perkins, 1968, 1970; Wand, 1970: Salah et al, 1975). Assuming that complete thermodynamic equilibrium is maintained, electron temperature variations are traceable to identical variations in the neutral species.

Variations in neutral temperature can arise from the semiduirnal tide or shorter period (< 4 hrs) gravity waves which presumably are randomly phased from day to day (Harper et al, 1976· Wand, 1976· Salah et al, 1975· Hooke 1969· Hines, 1965). The semiduirnal tide however is an unlikely candidate to explain our topside E_s observations since tidal gradients below 115 km are typically in the range $10^\circ/km \leq dT_n/dz \leq 20^\circ/km$, a value hardly comparable to the measurement, $dT_e/dz > 300^\circ/Km$.

If one is to ascribe the observed T_e variation to the influence of a changing neutral particle energy distribution, the more plausible source is the shorter period gravity wave which is identified with the wind shears giving rise

to sporadic-E layers (Hines and Colleagues, 1974). Even here, however, there are problems in firmly establishing the connection, particularly because the data base on the shorter period gravity waves is virtually non-existent at night and under conditions of sporadic-E.

Typically the mid-latitude incoherent scatter radar observations of T_i (assumed equal to T_n) have been confined to the daytime ionosphere because of lack of sensitivity to the reduced electron densities. Additionally, the radar measurements are influenced by T_i, T_e/T_i, ν_{in} (ion-neutral collision frequency), and the relative concentration and masses m_i of ionic species. In the referenced radar observations a nominal $\langle m_i \rangle$ = 30.5 a.m.u. was assumed. This assumption leads to a 2% error in the T_i determination if the molecular ion NO^+ (30 amu) is the only heavy charged species present (Salah et al, 1975). This sensitivity of the radar measurements to the m_i-distribution is particularly critical under E_s conditions where the dominant ions can be Fe^+(56 amu) and Mg^+(24 amu).

Another difficulty in establishing experimental support for a direct cause-effect relationship between gravity waves and our T_e observations is that our data would imply a vertical wavelength ~ 1 km. This is outside the detection capabilities of radars which typically integrate over a 2.5-3.0 km range and require 0.5-1.5 hrs. for a complete height profile of temperature. As no direct

measurements of gravity wave parameters were made during our experiment, we can only speculate on the characteristics of such a wave at the time of our observations.

b. Influences of Electron and Ion Distributions

In contrast to the proposition of total thermodynamic equilibrium and heating by gravity waves, we discuss here the effects of ion composition and plasma density on electron temperature within an E_s layer. We present the predictions of Gleeson and Axford (1967) and Hooke (1969), extend their calculations to a multiple ion-component plasma, and compare the results with our experimental observations.

Following the work of Gleeson and Axford (1967) it can be shown that an E_s-layer with two ionic species n_1 and n_2 (and associated recombination coefficients α_1 and α_2), has an altitude-dependent temperature differential between electrons and neutrals given by

$$T_e - T_n = \frac{\frac{3}{2}kT'_e + \left[\frac{1}{N_o}(n_1 + \frac{\alpha_2}{\alpha_1}n_2)\left(\frac{N_e}{N_o}\right) - \frac{5}{2}\right] kT_e}{L^*_{en}(\alpha_1 N_o)^{-1}\,(N_e/N_o)} \quad . \tag{12}$$

T'_e is defined as the energetic photoelectron "injection energy" (taken by Gleeson and Axford, and Hooke to be 8000° K), k is the Boltzmann constant, T_n is the neutral particle temperature, N_o is the ionospheric plasma

density in the absence of windshear, and

$$L^{*}_{en} = 1.55(10^{-15})N(N_2) + [5(10^{-18})T_e - (10^{-15})]N(O_2) \quad (13)$$

is the electron-to-neutral loss rate in eV per second per $^{\circ}K$ with the densities of N_2 and O_2 given in number per cm^3. In establishing Eq. (12) it was assumed that $\alpha_1 >> \alpha_2$ and $(n_1)_o >> (n_2)_o$, that is $n_1 >> n_2$ in the absence of windshear. These assumptions are supported by experimental observations (Johnson, 1968; Narcisi, 1968) which show that $N_o (\equiv (n_1)_o)$ is primarily a molecular ion combination of mean mass near 30 amu (e.g., NO^+ and O_2^+) with a recombination coefficient

$$4.2(10^{-7})(300/T_e)^{\left(.85^{+.25}_{-.15}\right)} \leq \alpha_1 \leq 7.5(10^{-7})\,(300/T_e)\,cm^2\,sec^{-1}$$

(Oppenheimer and Brace, 1976; Oppenheimer, et al, 1976; Torr, et al, 1976). The second ionic species n_2 is atomic, observed within E_s layers as a metallic (primarily Fe^+ and Mg^+) with a very small radiative recombination rate, $\alpha_2 \sim 3(10^{-12})\ cm^2\,sec^{-1}$ (Biondi, 1972).

If only molecular ions are present Eq. (12) becomes

$$T_e - T_n = \frac{\frac{3}{2}kT'_e + \left[\left(\frac{N}{N_o}e\right)^2 - \frac{5}{2}\right]kT_e}{L^{*}_{en}(\alpha N_o)^{-1}(N_e/N_o)} \quad . \quad (14)$$

Figure 5 presents the solutions to Eq. (14) for altitudes 100, 115, and 130 km, $T_n = 200^{\circ}K$ and $400^{\circ}K$, $\alpha N_o = 3(10^{-2})\ sec^{-1}$ and $(3/2)kT'_e = 1eV$.

Table 1. ALTITUDE DISTRIBUTIONS OF MOLECULAR NITROGEN

Altitude [Km]	N_2 Density [cm^{-3}]		
	I	II	III
100	$2(10^{12})$	$2.4(10^{12})^*$	$\geq 2.5(10^{12})^*$
115	$4.4(10^{11})$	$6.2(10^{12})^*$	$\geq 3.4(10^{12})$
130	$9.5(10^{10})$	$1.6(10^{11})$	$9.4(10^{10})$

The calculations assume the molecular nitrogen densities shown in column I of Table 1; these densities result from a fit to the original solutions of Gleeson and Axford (1967) at the same altitudes. For comparison, the Table shows two other N_2 distributions. The entries in column II have been taken from Dalgarno, et al (1967); they represent a modified Jacchia 1964 model for quiet, undisturbed, mid-latitude conditions during July 1963 at 1900 EST. (When measured in terms of diurnal, seasonal and solar-cycle influences, these conditions identify reasonably well with the period of our launch.) In column III are the rocket-borne observations of Hedin, et al (1964) at White Sands Missile Range on 6 June 1963 at 0730 MST. (The asterisk in columns II and III identify extrapolated values.)

At the altitudes in question we have neglected the electron energy losses to molecular oxygen. With $N(O_2) \leq 0.2N(N_2)$ and $T_e \leq 500^\circ K$, Eq. (13) shows this to be a reasonable assumption for simplifying the calculations and

subsequent discussions.

The minima in the family of curves shown in Fig. 5 and derived from Eq. (14) occur at a critical density ratio $(N_e/N_o)_c$ given approximately by

$$\left(\frac{N_e}{N_o}\right)_c = \sqrt{\frac{3T_e'}{2T_n}} \quad . \tag{15}$$

The prediction for the existence of a temperature minimum within an E_s-layer of molecular ions means that as one moves into an E_s-layer from the depleted regions outside (T_e-T_n) should decrease as N_e/N_o increases. If the layer were sufficiently intense so that $(N_e/N_o)_{peak} > (N_e/N_o)_c$, the difference (T_e-T_n) would achieve a minimum at the critical density ratio and then begin to increase as N_e/N_o increased toward the peak of the layer. Care must be exercised in evaluating the significance of this prediction, particularly since high recombination losses may prevent the development of a purely molecular ion E_s-layer with $(N_e/N_o)_{peak} > 7$. A more realistic approach includes metallic ions within the layer.

To demonstrate the effects of metallic ions on E_s-layer temperatures we assume an ion distribution that conforms to

$$n_1 = N_o + \delta(N_e-N_o) \tag{16}$$

and

$$N_e = n_1 + n_2 \tag{17}$$

where appropriate selection of δ will allow either an enhancement ($\delta>o$) or depletion ($\delta<o$) of the molecular species with the layer. With these assumptions Eq. (12) becomes

$$T_e - T_n = \frac{\frac{3}{2}\, kT'_e + \left[\left\{1 + \lambda\left(\frac{N_e}{N_o} - 1\right)\right\}\frac{N_e}{N_o} - \frac{5}{2}\right] kT_e}{L^*_{en}\ (\alpha_1 N_o)^{-1}\quad (N_e/N_o)} \tag{18}$$

where $$\lambda \equiv \delta\left(1-\frac{\alpha_2}{\alpha_1}\right) + \frac{\alpha_2}{\alpha_1} \quad . \tag{19}$$

Solutions to Eq. (18) are shown for four cases in Fig. 6 where the running parameter λ demonstrates the effects of ion distribution ($\lambda\approx\delta$ for realistic values of α_2/α_1 ($\approx 10^{-6}$)).

The case $\lambda=1$ represents a purely molecular ion layer where a temperature minimum occurs at modest values of N_e/N_o. As λ decreases, the contribution of metallic ions to the total plasma density increases, and the location of the temperature minimum shifts to higher values of N_e/N_o according to the approximate relationship

$$\left(\frac{N_e}{N_o}\right)_c = \sqrt{\frac{1}{\lambda}\ \frac{3T_e}{2T_n}}\ , \tag{20}$$

Equation (20) applies for all $\lambda>o$. For $\lambda\leq o$ there is no minimum.

The case $\lambda=o$ represents the transition between molecular enhancement ($\lambda>o$) and molecular depletion

(λ<o) within the layer. The latter case is perhaps more representative of an actual E_s condition, being in agreement for example with Young, et al (1967) who found molecular ion concentrations greatly reduced within the layer. In contrast to the case of the pure molecular-ion layer, this suggests that predominately metallic layers with molecular species depleted by enhanced electron recombination should have the temperature minimum identified with the layer peak.

To compare the predictions of theory with our results, the upleg-E_s profile has been smoothed and presented at the bottom of Fig. 7 in the N_e/N_o vs Z format. N_o has been defined by the I_B-level in Fig. 3 in the region $107.5 \leq Z \leq 107.7$. This definition and the analysis procedure detailed in Section 2 yields $N_o = 2.2(10^4) cm^{-3}$.

The difference between measured values of T_e and an assumed neutral temperature of 300° K is plotted at the top of Fig. 7, with open circles representing upleg data and solid circles representing downleg values normalized appropriately to N_e/N_o. The error bars indicate best estimates of inaccuracy in the T_e values. The estimate stems from careful scrutiny of Maxwellian fits to retarded electron currents in the region $(\chi - 1) < \chi \leq (\chi_f + 4)$. The subscript "f" identifies the floating potential. The lowest measured value of T_e was 340° K and the largest estimated error was ± 15° K. With the P^3 procedure

stabilizing probe surface conditions no error was identified with possible measurement distortion by contamination effects. The selection $T_n = 300^\circ K$ is arbitrary, but over the altitude range 106 to 108 Km it is consistent with the lower thermospheric temperature results reported by Salah and Wand (1974).

The top of Fig. 7 includes the predictions of Eq. (18) for the parametric cases detailed in Table 2. Curve "a" is the result of applying the parameters and loss terms used by Gleeson and Axford (1967). The G-A entry in Table 2 identifies the extrapolated density distribution which follows from Table 1, column I.

Table 2. PARAMETERS SELECTED FOR TWO-SPECIES PREDICTIONS WITH $\lambda = 0$ AND $T_n = 300^\circ K$

Parameter	CURVE	
	a	b
$\alpha_1 N_o [sec^{-1}]$	$3(10^{-2})$	$1.2(10^{-2})(300/T_e)$
$[N_2]$	G-A	0.2 G-A
L^*_{en}	Eq. (13)	Eq. (21)
$\frac{3}{2}kT'_e[eV]$	1	2.0

Curve "b" represents adjustments in the parameters in "a". As detailed in Table 2, the adjustments include:

i) The use of a more recent analytic representation for electron neutral losses (Banks and Kocharts, 1973; Dalgarno, 1969) through N_2 rotational excitation. This new loss term is given by

$$L^{*}_{en} \equiv 2.0(10^{14})\ N(N_2)/\sqrt{T_e} \qquad (21)$$

with an uncertainity of a factor of 2.

ii) The increase of the electron injection energy $\frac{3}{2}kT'_e$ from 1eV to 2eV. This allows the upper bound on T'_e to extend beyond the 1.5eV cut-off identified with vibrational excitation of N_2 in the energy cascading process of photoelectrons (Dalgarno, et al, 1963; Dalgarno, et al, 1967; Timothy, et al, 1972). When one includes energy transfer to thermal electrons from vibrationally excited N_2, the greatest upper bound on T'_e extends as high as 5eV (Dalgarno, et al, 1963).

iii) A reduction in $\alpha_1 N_O$ from $3(10^{-2})\ sec^{-1}$ to $1.2(10^{-2})sec^{-1}$ in order to reflect a value more in keeping with experimental conditions (i.e., $\alpha_1 = 5.5(10^{-7})\ cm^3 sec^{-1}$, $N_O = 2.2(10^4)cm^{-3}$). Case "b" also reflects temperature dependence in the reaction rate coefficient α_1, in accordance with Biondi [1972], Torr, et al [1976], and Oppenheimer [1976].

iv) An adjustment in molecular nitrogen densities which brings model predictions within the range of our measurements.

In evaluating the theoretical curves, we note that each could have been generated from an unlimited number of parametric combinations. This lack of uniqueness in the model predictions imposes some constraints on conclusions drawn from comparison with experimental results. For example, the choices for T_e' and N_2 in Case "b" were selected to improve the fit between theory and experiment. These same parameters could be justifiably altered to produce solutions that are in lesser agreement with our results. (We note that the N_2 density of Case "b" represents an excursion which goes beyond existing information on neutral density variations at 105 km (See e.g. Faucher and Morrissey, 1971).) The quantitative agreement is therefore qualified because of an incomplete determination of all existing conditions.

We note however, that the most significant feature of the data is the steep gradient in electron temperature. The measured temperature gradient is real, and its relationship to a Gleeson-Axford model is the substance of Figure 7.

V. SUMMARY

The first ionospheric application of a newly-developed pulsed-plasma-probe is described in an electron temperature study of mid-latitude sporadic-E. The major new result was the definitive observation of an electron temperature gradient across the layers. Layer-peak and bottom-side values of T_e were approximately equal at 340°K but the topside of each layer showed temperature increasing to 515°K as the electron density decreased with altitude to the undisturbed ambient E-region value.

The electron temperature observations were compared with the theoretical predictions of gravity wave heating as well as with predicted effects of variations in both electron density and ion composition within the sporadic-E layer itself. Within the framework of plausible atmospheric variations neither mechanism could be uniquely identified with the observations. Final and conclusive analyses require simultaneity in the measurements of N_e, T_e, T_i, M_i, and T_n with spatial resolution much greater than currently available.

ACKNOWLEDGMENTS

The work was carried out with the support of the Office of Naval Research and the able assistance of Mr. L. Kegley. We express our sincere thanks to Mr. C. Y. Johnson for his assistance in data handling procedures and his many discussions of results.

REFERENCES

Aubrey, M., Blanc, M., Clauvel, R., Taieb, C., Bowen, P.J., Norman, K., Wilmore, A.P., Sayers, J. and Wager, J.H., Some rocket results of S poradic-E, Radio Sci. 1, 170 (1966).

Axford, W. I., Wind Shear Theory of the Formation of Temperate Zone Sporadic-E Layers, Spac. Res. 7, 126, 1967.

Banks, P. N., and G. Kocharts, in Aeronomy, Part B, p. 268, Academic, New York, 1973.

Biondi, M. A., Charged particle recombination processes, in Reaction Rate Handbook, DNA 1948H, P. 16-1, edited by M. H. Bortner and T. Baurer, DASIAC, GE TEMPO, Santa Barbara, Ca., 1972.

Boyd, R. L. F., Langmuir probes on spacecraft, in Plasma Diagnostics, edited by W. Lochte-Holtgreven (North Holland, Amsterdam, 1968) p. 732.

Carru, H., M. Petit, G. Vasseur, and P. Waldteufel, Resultats conospheriques obtenus par diffusion de Thompson, Ann. Geophys. 23, 455 (1967a).

Carru, H., M. Petit, and P. Waldteufel, Masuers de temperatures electroniques a et ioniques par diffusion incohérente, J. Atmos. Terr. Phys. 29, 351 (1967b).

Chen, F. F., Electric probes, in Plasma Diagnostic Techniques, edited by R. H. Huddlestone and S. L. Leonard (Academic, New York, 1965), p. 113.

Dalgarno, A., Inelastic collisions at low energies, Can. J. Chem. 47, 1723, 1969.

Dalgarno, A., M. B. McElroy, and J. C. G. Walker, The diurnal variation of ionospheric temperatures, Planet Space Sci. 15, 331, 1967.

Dalgarno, A., M. B. McElroy, and R. J. Moffett, Electron Temperatures in the ionosphere, Planet Space Sci. 11, 463, 1963.

Evans, J. V., Electron temperature and ion composition in the F_1 region, J. Geophys. Res. 72, 3343 (1967).

Faucher, G. A., and J. F. Morrissey, Atmospheric density measurements in the 70-115 kilometer region, J. Geophys. Res. 76, 4145, 1971.

Gleeson, L. J., and W. I. Axford, Electron and Ion Temperature Variations in Temperate Zone S poradic-E Layers, Planet. Space Sci. 15, 123, 1967.

Harper, R. M., R. H. Wand, C. J. Zumlatti, and D. T. Farley, E region ion drifts and winds from incoherent scatter measurements at Arecibo, J. Geophys. Res. 81, 25 (1976).

Hedin, A. E., C. P. Avery and C. D. Tschetter, An analysis of spin modulation effects on data obtained with a rocket-borne mass spectrometer, J. Geophys. Res. 69, 4637, 1964.

Hines, C. O., Dynamical heating of the upper atmosphere, J. Geophys. Res. 70, 177 (1965).

Hines, C. O., and Colleagues, The Upper Atmosphere in Motion, Geophysical Monograph (American Geophysical Union, Wash., D.C., 1974).

Hirao, K., and K. Oyama, A critical study of the reliability of electron temperature measurements with a Langmuir probe, J. Geom. Geoelectr. 24, 415, 1972.

Holmes, J. C., and E. Szuszczewicz, A versatile plasma probe, Rev. Sci. Instr. 46, 592, 1975.

Hooke, W. H., Electron, Ion and Neutral-Gas Temperatures in Temperate Latitude Sporadic-E Layers, Planet. Space Sci. 17, 737, 1969.

Hooke, W. H., Radar Thomson scatter observations of E-region temperatures interpreted as revealing reversible heating by atmospheric tides, J. Geophys. 74, 1870 (1969b).

Jacchia, L. G., Res. Space Sci., Smithson. Astrophys. Obs., Spec. Rep. 170, 1964.

Johnson, C. Y., E_s structure and composition above White Sands, New Mexico, in Proceedings of Second Seminar on the Cause and Structure of Temperate Latitude Sporadic-E, S. Matshushita and E. K. Smith, Chairmen, (Conference Proceedings, 19-22 June 1968, Vail, Colorado), p. III-2.

Laframboise, J. G., Theory of spherical and cylindrical Langmuir probes in a collisionless, Maxwellian Plasma at rest, Rep. 100 Inst. of Aerospa. Stud., Univ. of Toronto, Toronto, Ont., 1966.

Layzer, D., Theory of midlatitude sporadic E, Radio Science 7, 385, 1972.

Macleod, M. A., Sporadic-E Theory 1. Collision-Geomagnetic Equilibrium, J. Atmos. Sci. 23, 96, 1966.

Matsushita, S., and E. K. Smith (Co-Chairmen), Third Seminar on the cause and structure of temperate latitude sporadic E, (Logan, Utah; Sept. 1971), in special issue Radio Science 7, 345-432, 1972.

Matsushita, S., and E. K. Smith (Guest Editors), Conference on recent advances in the physics and chemistry of the E region, (Boulder, Colorado; Aug. 1974), in special issue Radio Science 10, 229-418, 1975.

Narcisi, R. S., Processes associated with metal-ion layers in the E-region of the ionosphere, in Proceedings of Second Seminar on the Cause and Structure of Temperate Latitude Sporadic-E, S. Matsushita and E. K. Smith, Chairmen, (Conference Proceedings, 19-22 June 1968, Vail, Colorado), p. III-3; also in Space Research VIII, edited by A. P. Mitra, L. G. Jacchia, and W. N. Newman, p. 360, North-Holland, Amsterdam, 1968.

Oppenheimer, M., and L. Brace, Recombination rate coefficient of NO^+ from thermosphere daytime photochemistry, Trans. Am. Geophys. U. 57, 297, 1976.

Oppenheimer, M., A. Dalgarno, K. Kirby-Docken, and G. A. Victor, Ion chemistry of the datime thermosphere, J. Geophys. Res. (1976, in press).

Salah, J. E., Evans, J.V., and R. H. Wand, E-region temperature measurements at Millstone Hill, J. Atm. Terr. Phys. 37, 461 (1975).

Salah, J. E. and R. H. Ward, Tides in the lower thermosphere at mid-latitudes, J. Geophys. Res. 79, 4295, 1974.

Smith, L.G., Summary and conclusions from the Estes Park sporadic-E seminar 2. Rocket measurements, Radio Sci. 1, 170, 1966.

Sturges, D. J., An Evaluation of Ionospheric Probe Performance-I Evidence of Contamination and Clean-Up of Probe Surfaces, Planetary & Space Sci. 21, 1029, 1973.

Szuszczewicz, E. P., Area Influences and Floating Potentials in Langmuir probe measurements, J. Appl. Phys. 43, 874, 1972.

Szuszczewicz, E. P., and J. C. Holmes, Surface contamination of active electrodes in plasmas: Distortion of conventional Langmuir probe measurements, J. Appl. Phys. 46, 5134, 1975.

Szuszczewicz, E. P. and J. C. Holmes, A pulsed plasma probe technique for simultaneous in-situ measurements of density, temperature, density fluctuation power spectra and ambient electric fields, in Effect of the Ionosphere on Space Systems and Communications, edited by J. M. Goodman, p. 445, U. S. Gov't. Printing Office, 1976a.

Szuszczewicz, E. P. and J. C. Holmes, Reentry plasma diagnostics with a pulsed plasma probe, AIAA Paper No. 76-393, 1976b.

Timothy, A. F., J. G. Timothy, and A. P. Willmore, the ion chemistry and thermal balance of the E- and lower F-regions of the daytime ionosphere: An experimental study, J. Atmosph. Terr. Phys. 34, 969, 1972.

Torr, D.G., M. R. Torr, J.C.G. Walker, L. H. Brace, H. C. Brinton, W. B. Hanson, J. H. Hoffman, A. O.Nier, and M. Oppenheimer, Recombination of NO^+ in the ionosphere, Geophy. Res. Let. 3, 209, 1976.

Wand, R. H., Semidiurnal tide in the E-region from incoherent scatter measurements at Arecibo, Radio Sci. 11, 641 (1976).

Wand, R. H., and F. W. Perkins, Radar Thomson scatter observations of temperature and ion-neutral collision frequency in the E-region, J. Geophys. Res. 73, 6370 (1968).

Wand, R. H., and F. W. Perkins, Temperature and composition of the ionosphere: diurnal variations and waves, J. Atm. Terr. Phys. 32, 1921 (1970).

Wehner, G., and G. Medicus, Reliability of probe measurements. J. Appl. Phys. 23, 1025, 1952.

Wharton, L. E., and W. R. Hoegy, Current to moving spherical and cylindrical electrostatic probes, NASA x-621-71-276, June 1971.

Whitehead, J. D., Survey of Sporadic-E processes, Space Res. 7, 90, 1967.

Young, J. M., C. Y. Johnson, and J. C. Holmes, Positive ion composition of a temperature-latitude sporadic-E layer as observed during a rocket flight, J. Geophys. Res. 72, 1473, 1967.

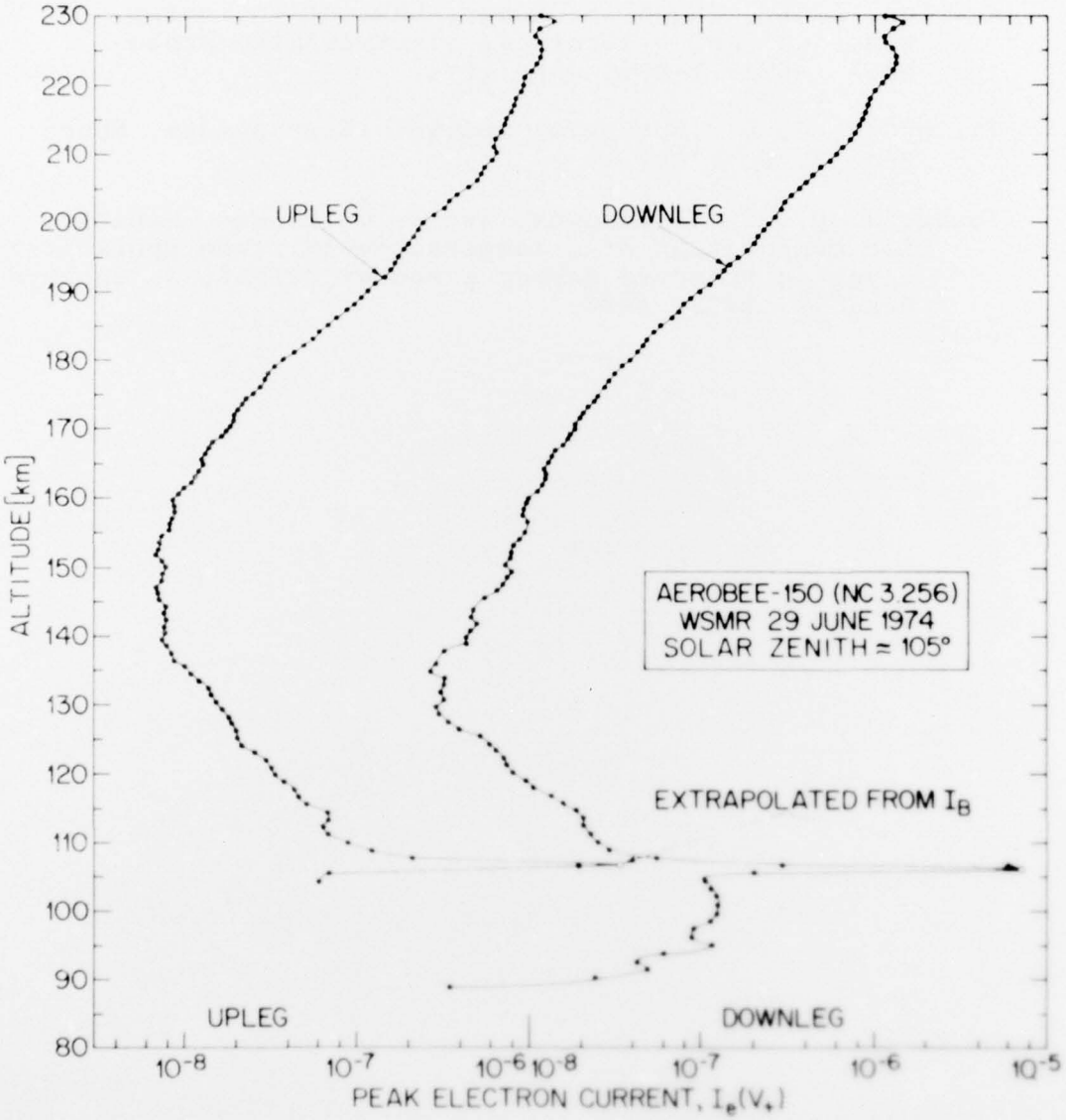

Fig. 1 — Relative electron density profiles determined by probe currents collected at $V_p = V_+ = +3$ volt. Note the shifted current scales for the up- and downleg portions of the flight.

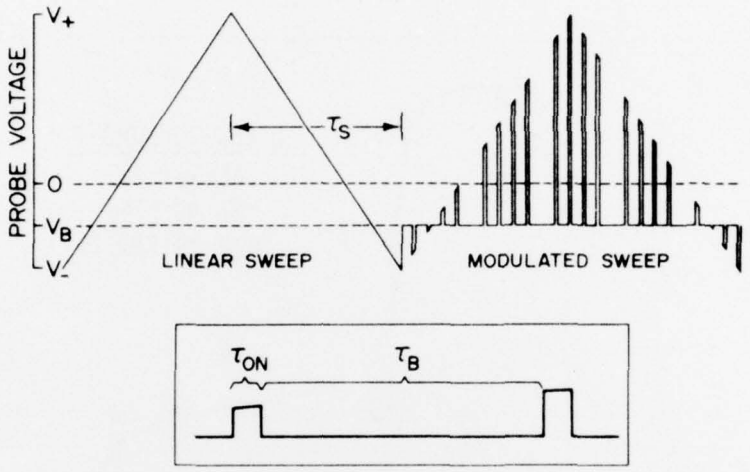

Fig. 2 — Continuous and modulated sweep modes of probe operation. The continuous, linear sweep represents the conventional approach while the modulated sweep schematically presents the procedure of the pulsed plasma probe (P^3) technique. The pulses were applied at a 512 sec^{-1} rate, allowing for 193 pulses during the voltage sweep between V_- and V_+. The inset is an expanded scale of two adjacent pulses.

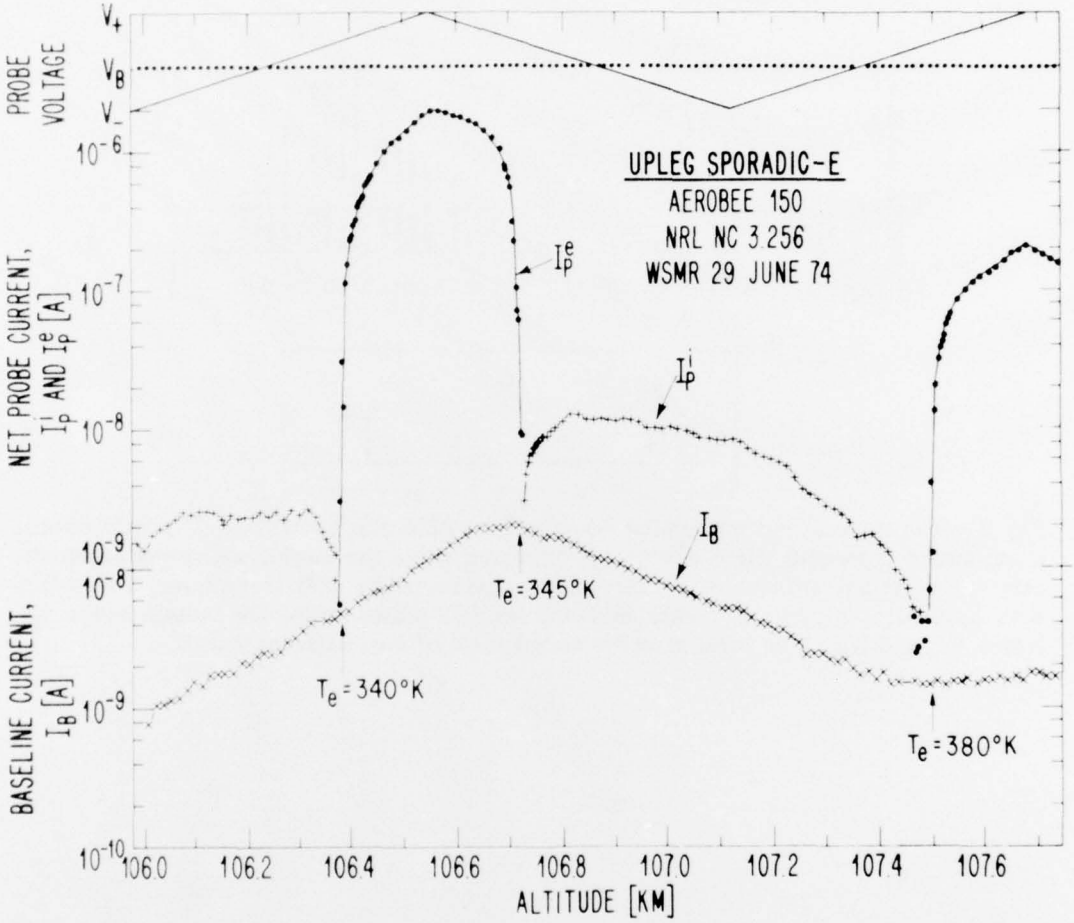

Fig. 3 — Expanded view of probe voltages and currents as the payload traversed the E_s-layer on the upleg portion of the flight. The values of T_e were identified in space and time with the floating potential of the I-V characteristics from which they were derived.

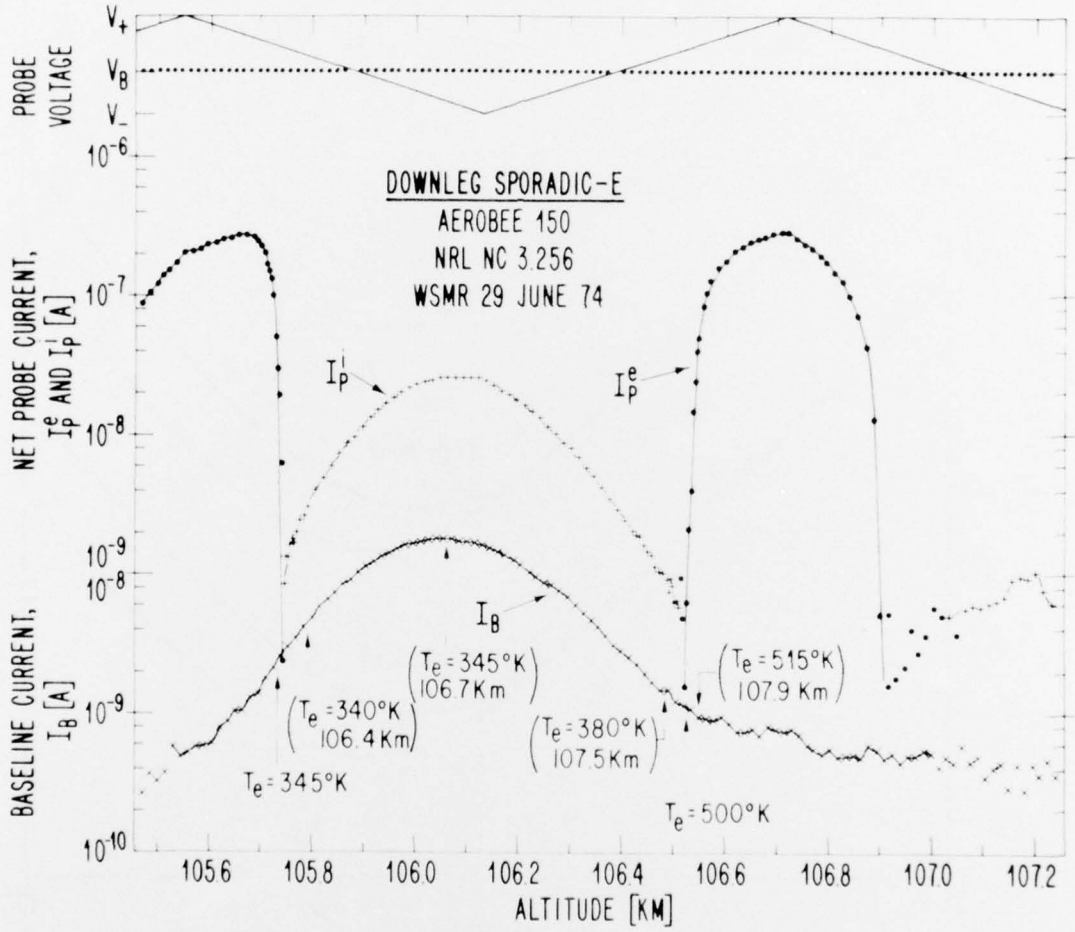

Fig. 4 — Expanded view of probe voltage and currents yielding the indicated temperature measurements of 345°K and 500°K at the bottom- and topside of the downleg E_s-layer. The values T_e shown in parentheses were determined in the upleg layer and superimposed on the downleg profile by identification with identical ratios of N_e/N_e^{peak}. Values of I_B represent the density profile within the layer.

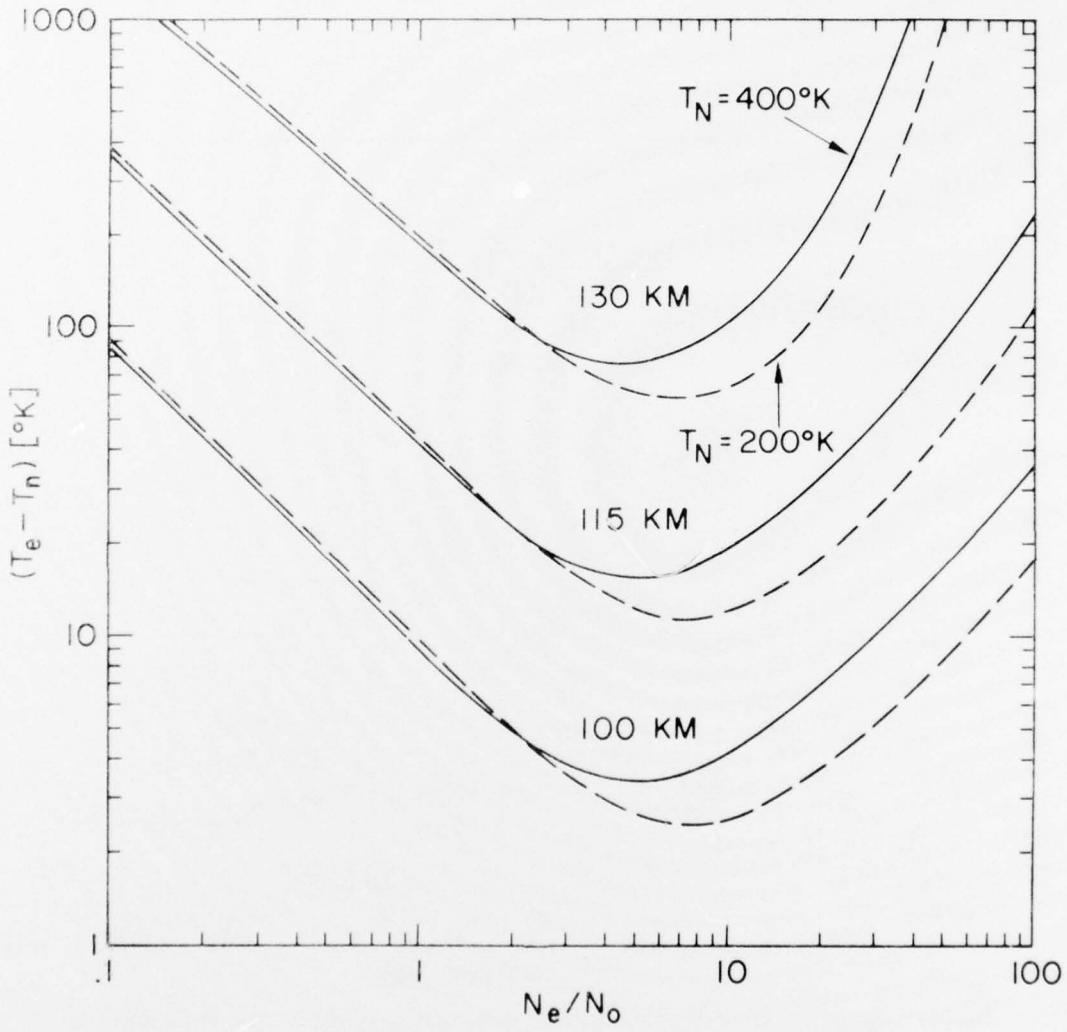

Fig. 5 — Dependence of $(T_e\text{-}T_n)$ on altitude and electron density within an E_s-layer when $\alpha N_o = 3(10^{-2})\text{sec}^{-1}$ and $T_e' = 8(10^3)°\text{K}$. Neutral densities are taken from Table 1, column I.

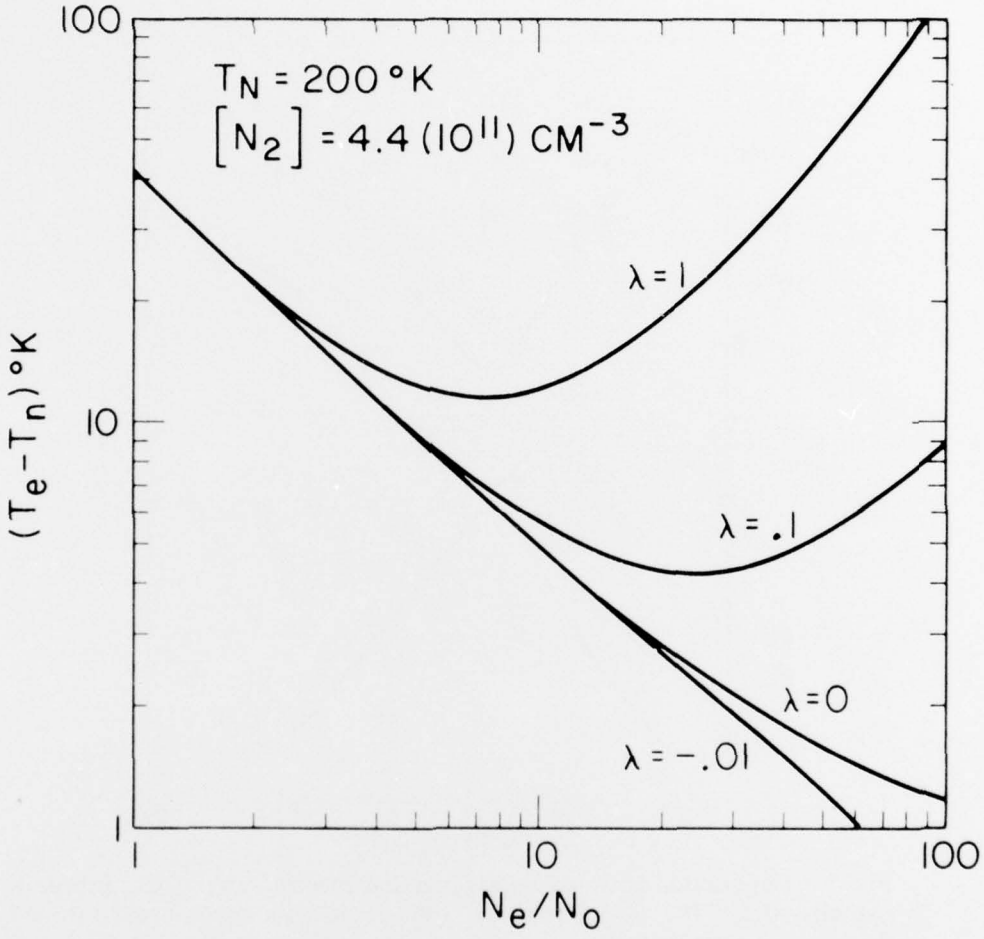

Fig. 6 — Dependence of temperature on ion composition within an E_s-layer. For $\alpha \ll 1$, $\lambda = +1$ identifies a purely molecular ion layer. As λ becomes less than +1 the contribution of metallics becomes increasingly more important in the total ion population. $\lambda < 0$ identifies metallic layers accompanied by molecular depletion.

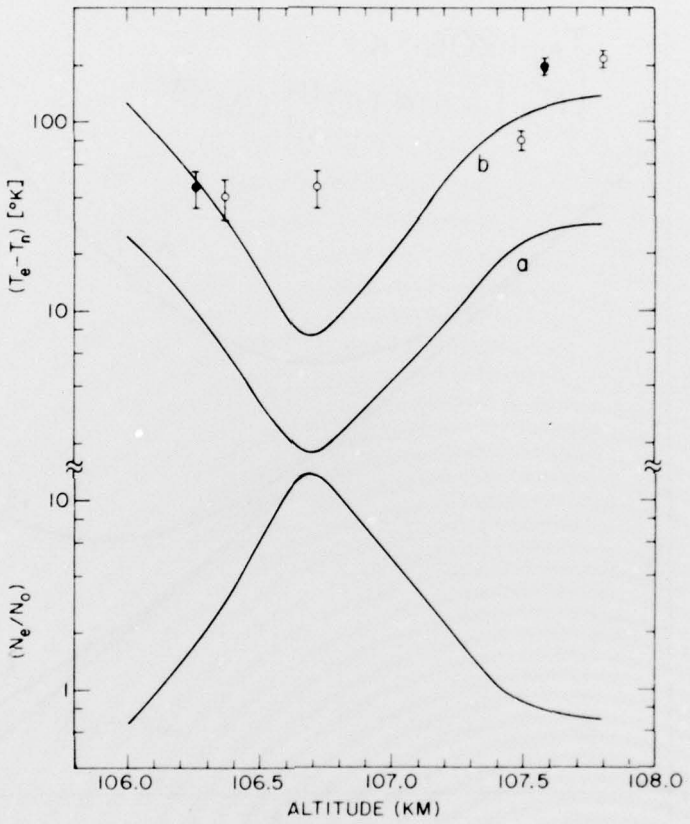

Fig. 7 — Comparison between experiment and theory. The N_e/N_o profile is experimental. The open-circle and solid-circle data present the up- and downleg T_e measurements, respectively. The difference $(T_e - T_n)$ assumes $T_n = 300°K$ across the layer. Conditions for theoretical curves a, and b, are presented in Table 2.